Collisionless perpendicular shocks - Applications to solar type II radio bursts and the Antares /alpha Sco/ radio emission

Klinkhamer, F.R.; Kuijpers, J.

Astron. Astrophys. 100, 291–301 (1981)

ASTRONOMY AND ASTROPHYSICS

Collisionless Perpendicular Shocks: Applications to Solar Type II Radio Bursts and the Antares (α Sco) B Radio Emission

F. R. Klinkhamer[1] and J. Kuijpers[2]

[1] Sterrewacht, Huygens Laboratorium, Wassenaarseweg 78, 2300 RA Leiden, The Netherlands
[2] Sterrekundig Instituut, Zonnenburg 2, 3512 NL Utrecht, The Netherlands

Received July 3, 1980; accepted March 13, 1981

Summary. We propose a model of a collisionless perpendicular ($v \perp B$) shock based on:

1. local marginal stability of ion-acoustic waves,
2. ion heating in supercritical shocks by a beam of reflected ions behind the shock proper.

We calculate a mean turbulence energy density in the shock.

Type II radio bursts of the Sun and their characteristic fine structures can be explained. The effective temperature of the ion-sound waves is substantially larger than the observed radio brightness temperature. Using the turbulent Bremsstrahlung mechanism for Langmuir waves the radio luminosity can be accounted for.

Finally we consider the observed radio emission from the Antares B companion star which is embedded in a stellar wind from the M supergiant. The available free energy in a single bow shock is far less than the observed radio luminosity. However, the estimated wind from the B star itself creates a secondary shock which is sufficiently energetic to account for the observed emission.

Key words: shock waves (collisionless) – radio star – Antares (αSco) B – solar radio bursts – mass loss

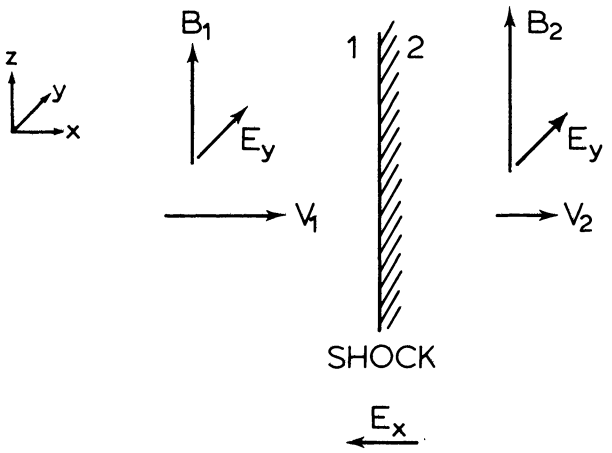

Fig. 1. Shock geometry and conventions. Our reference system is comoving with the shock which gives rise to the induction field E_y. Pre-shock quantities have an index 1, post-shock quantities have an index 2. The field E_x is only present in the shock front and is responsible for an electric current in the negative y direction (see text Sect. 1)

1. Introduction

In ordinary gasdynamics a shock typically has a thickness of a mean collisional free path of a gas particle. The bow shock of the Earth in the solar wind (e.g. Formisano, 1977; Greenstadt and Fredricks, 1979) on the contrary has a much smaller thickness. Collisions, being the mechanism to randomize the kinetic energy in the front of an ordinary shock, must be less effective than other processes, presumably of a plasma character, in the Earth's bowshock. Many aspects of collisionless shocks (simply 'shocks' henceforth) are reviewed by Sagdeev (1966), Tidman and Krall (1971, TK) and Biskamp (1973). We will discuss socalled (stationary) laminar, plane and perpendicular shocks, where quantities as density and magnetic field vary gradually, apart from the microturbulence on a scale much smaller than the shock thickness. In turbulent shocks the whole structure is strongly variable, both in space and time. Our reference-system will be moving along with the shock front; Figure 1 introduces the configuration considered, with the magnetic field perpendicular to the flow velocity, ($B \perp v$) and some of the conventions used.

Send offprint requests to: F. R. Klinkhamer

Now we shall briefly discuss some general aspects of collisionless shocks relevant to this paper. Best understood is the resistive shock, where anomalous resistivity is the 'braking' mechanism; in a plasma with $\beta \equiv nKT/(B^2/8\pi) < 1$ the shock thickness is of order c/ω_{pe} (Biskamp, 1973). A physically consistent picture is the following (Cairns, 1978): in the shock frame (Fig. 1) a constant induced electric field is present in the y-direction $E_y = v_1 B_1/c$ (Tidman and Krall, 1971). The drift velocity of the electrons, which is proportional to E/B, is reduced in the shock because of the increasing magnetic field strength. However, the ion drift velocity is not reduced on the scale of the shock since the ion Larmor radius is larger than the shock width: an electric field E_x is created in the negative x-direction which slows down the ions. This electric field also induces a drift of the electrons in the y-direction and therefore an electric current which in turn gives rise to the magnetic field change from which we started. Further the relative drift between electrons and ions in the y-direction leads to an instability for ion-acoustic waves which tend to limit the drift and to heat the electrons, giving rise to an anomalous resistivity.

For Mach numbers M_A (relative to the Alvén velocity) larger than a critical value (2–3), however, the simple two-fluid

model breaks down, because the anomalous resistivity of the electrons cannot stabilize the ion density profile anymore (Galeev, 1976) and an extra effective ion viscosity is needed. Ions reflected on the potential rise in the shock are essential to this viscosity (Biskamp, 1973). Sherwell and Cairns (1977) showed that these reflected ions, which again are turned back towards the shock by the magnetic field and accelerated by the induction field (E_y in Fig. 1), contain a significant amount of free energy stored in their non-Maxwellian distribution function (i.e. accelerated beam) which they dissipate behind the shock proper. By this mechanism the ions, which are less sensitive than the electrons to heating by the microturbulence in the shock, can be heated to their expected Rankine-Hugoniot temperature far behind the shock.

Two remarks on the Rankine-Hugoniot (RH) relations relevant to our discussion:

1. a priori it is unclear whether the RH-relations, which are derived from Maxwell distributions before and behind the shock (TK), can be applied on the scale of the *collisionless* shock or only over larger distances, of order of the mean free path, and

2. if electrons and ions have different degrees of freedom (perhaps if heated by microturbulence in the shock) an extra equation on the ion heating is needed to derive the RH-relations (Sanderson and Uhrig, 1978).

In this paper we will discuss perpendicular shocks in a $\beta \leqq 1$ plasma. Oblique shocks or a high β result in oscillatory structures (cf. solitons): anomalous resistivity remains too weak, because many instabilities require of the drift velocity to exceed some fraction of a thermal speed ($v_D > \ldots v_{tj}$); this might be impossible to satisfy in an oblique situation ($\Delta B_\perp \propto v_D$ small) or if $\beta > 1$ (v_{tj} large). These oscillatory structures may decay on numerous waves (Galeev, 1976) and a turbulent character of the shock results.

In Sect. 2 we discuss a model to derive the energy density of the turbulence and the thickness for a collisionless shock, which we use to make (Sect. 3.1) some estimates on the expected radio emission, which in turn are compared with the observations of type II radio bursts of the Sun and with the enigmatic radio emission of Antares B (Sects. 3.2. and 3.3.). Section 4 contains the conclusions. We will use Gaussian cgs units and common notations as $T_6 = T/10^6$ K. A list of symbols is presented at the end of the paper.

2. Collisionless Perpendicular Shock

2.1. Model

We extend the concept of a resistive shock to supercritical Mach numbers, assuming that ion reflection takes care of the necessary heating of the ions (see Sect. 1). Too large shock velocities are excluded ($M_A < 43$), otherwise 1. the electron Larmor radius would not be smaller than the experimentally observed shock thickness of order c/ω_{pe} and 2. the reflected ions would not be a small fraction of the mainstream ions, which make the shock.

To calculate the structure of the (ion-acoustic) resistive shock Manheimer and Boris (1972, MB) used the concept of local marginal stability: We assume that the microscopic plasma relaxation time scales are so small in comparison with the shock width transit time that the plasma is marginally stable with respect to the relevant plasma instabilities. This condition determines the distance over which the given magnetic field change occurs, which in turn determines the required effective collision frequency, which finally determines the required wave level.

Detailed computations by Lemons and Gary (1978) show that if $T_e \gg T_i$ in the shock the ion-acoustic instability is dynamically the most important out of seven electrostatic and electromagnetic modes (see also Papadopoulos, 1977 and Galeev, 1976). In our case the electrons are preheated in the so-called 'foot', a region where the reflected ions are turned around (e.g. TK) so that T_e becomes larger than T_i. Clear evidence for ion-acoustic waves in perpendicular earth bow shock measurements was found by Rodriguez and Gurnett (1975). Calculations of shock widths using marginal stability of current-driven electrostatic waves compare well with the observations (Morse and Greenstadt, 1976).

Because the small fraction of reflected ions does not change the growth rate of the ion-acoustic instability fundamentally (see Sect. 2.3.), we derive the same equation as MB from the condition of marginal stability ($\gamma \simeq 0$):

$$\frac{c}{4\pi ne}\frac{dB}{dx} = \left(\frac{KT_e}{2m_i}\right)^{1/2} q^{1/2}\left[1+\left(\frac{m_i T_e^3}{m_e T_i^3}\right)^{1/2}\exp\left(-\frac{q}{4}\frac{T_e}{T_i}\right)\right], \tag{1}$$

with

$$q \equiv 1+\left(1+\frac{12\,T_i}{T_e}\right)^{1/2} \simeq 2.$$

In order to obtain the shock thickness L_s (parametrized by $l = L_s\omega_{pe1}/c$);

1. we approximate the derivative in Eq. (1) by $\Delta B/L_s$ (cf. Morse and Greenstadt, 1976)

2. we estimate n_2, T_2 after the shock and ΔB with the RH relations for strong shocks (for small Mach numbers the end result (6) differs slightly from that obtained by using the correct RH relations). Thus in Eq. (1) we use mean values (with tilde) $K\tilde{T}_e = 3/32\, m_i v_1^2$, $\tilde{n} = 5/2\, n_1$, $\Delta B = 3B_1$.

3. as explained above we assume that by the micro-instability the electrons will have attained the RH temperature just behind the shock, whereas the ions in the shock will only be heated by:

(i) adiabatic compression:

$$\frac{T_{i_2}}{T_{i_1}} = (n_2/n_1)^{2/S_i}, \tag{2}$$

with S_i the number of degrees of freedom; for the mainstream ions we take $S_i = 3$.

(ii) resistivity heating by the ion-acoustic turbulence (Caponi and Davidson, 1973):

$$\frac{3}{2}nv\frac{dKT_i}{dx} = nm_e v_D^2 \nu^*\left(\frac{c_s}{v_D}\right). \tag{3}$$

With $v_D \sim c_s$ locally and the effective electron collision frequency ν^* required to maintain a shock thickness L_s (MB, printing error; Biskamp, 1973)

$$\nu^* = \frac{\omega_{pe}^2}{c^2} v_A L_s, \tag{4}$$

Eq. (3) gives for the resistive heating

$$(\Delta KT_i)_{\text{res}} \simeq 2.63\, m_e v_D^2 \frac{\omega_{pe_1}^2}{c^2} M_A^{-1} L_s^2. \tag{5}$$

We add this temperature rise (with $v_D \simeq \tilde{c}_s$ i.e. marginal stability) to T_{i2} from Eq. (2) and with $KT_{e2} \simeq 3/16\, m_i v_1^2$ we have an estimate for the ratio T_e/T_i in the shock from:

$$\frac{T_{e2}}{T_{i2}} = 0.074\,\theta, \tag{6a}$$

$$\theta \equiv \left[\left(\frac{1}{2M_A^2}\right)\left(\frac{\beta T_i}{T_e}\right)+1.4\,10^{-5}\,\bar{l}^2\right]^{-1},$$

where

$$L_s \equiv \frac{lc}{\omega_{pe_1}},\quad \bar{l}=lM_A^{-1/2}.$$

Note that we used the identity $KT_{i1}/m_i v_1^2=\beta T_{i1}(2\,T_{e1}M_A^2)^{-1}$.

Finally with this ratio and the mean values from 1. and 2. Eq. (1) leads to

$$\bar{l}\simeq 170\,M_A^{-3/2}\,[1+0.31\,\theta^{3/2}\exp(-1.9\,10^{-2}\theta)]^{-1}, \tag{6b}$$

where we have approximated $T_e/T_i\simeq 0.5\;T_{e2}/T_{i2}$ requiring $\theta \gg 27$.

This condition together with Eq. (6a) then leads to the following restrictions ($T_{i1}=T_{e1}$)

$$\beta \ll 0.07\,M_A^2,$$

$$\bar{l}^2 \ll 26^2.$$

The numerical value of $\bar{l}$ can be derived from Eqs. (6a, b). Neglecting the β term in Eq. (6a), which is justified if

$$\beta \ll 1.1\,10^{-4}\,M_A^2\bar{l}^2$$

one finds that $5<\bar{l}<15$ for $10>M_A>2$. As a characteristic value in the applications we shall use $l\simeq 10$.

With the shock thickness calculated above, the effective electron collision frequency ν^* from Eq. (4) and an expression in terms of the turbulence energy density (Sagdeev, 1972; Galeev, 1976).

$$\nu^*=\frac{\omega_{pe}W}{nKT_e}, \tag{7}$$

we arrive at an estimate of the energy density of the ion-acoustic turbulence in the shock

$$\frac{W}{nKT_e}=l\frac{v_A}{c}. \tag{8}$$

2.2. Conditions

In this paragraph we would like to mention the conditions of validity for our model, which are schematically

1. Mach number and β: $\beta\lesssim 1$ or $T_{10}\lesssim\frac{1}{3}\,(\omega_{ce}/\omega_{pe})^2$ in front of the shock;
$M<43$ if perpendicular
[$M\lesssim 3$ (?) if quasi-perpendicular]

2. orientation of the magnetic field (ϑ is the angle between v_1 and B_1):

$$\vartheta\gtrsim\frac{\pi}{2}-(m_e/m_i)^2 \text{ (perpendicular)}$$

($\vartheta\gtrsim 50^0$, "quasi-perpendicular" see discussion below)

3. $\omega_{ce}/\omega_{pe}\ll 1$ in the shock

4. c/v_A and $c/c_S\geqq 1000$.

The explanation is as follows:

1,2. For large shock velocities or high β the shock will be turbulent, that is non-stationary (e.g. Woods, 1971). In this respect relevant observations of the bow shock of the Earth are (Greenstadt and Fredricks, 1979):

(i) $\beta\lesssim 1$: electrostatic turbulence,

(ii) $M>3$: stronger turbulence than at lower Mach numbers,

(iii) $\vartheta\gtrsim 50^0$: (a) similar profile as the perpendicular shock, however with a thickness of $\sim c/\omega_{pi}$,

(b) the ion distribution function behind the shock is bimodal, just as for the perpendicular shock,

(c) if $\beta\gtrsim 8$ the magnetic field is non-stationary.

Experimentally we thus see a strong resemblance of the perpendicular shock with his more oblique colleague, but how must our calculations as presented in 2.1 be modified to include the quasi-perpendicular case?

(i) The RH relations used are quite insensitive to ϑ, as long as we take point (iii) below into account (TK., Figs. 1.5–1.7).

(ii) The ion-acoustic instability is independent of the magnetic field, as long as condition 3 holds.

(iii) The mean magnetic field in the x-direction is constant throughout the shock (TK), for 'B' we thus must read 'B_z'.

(iv) In the perpendicular case ions are partially heated by ions reflected on the potential rise. If $\vartheta<\frac{\pi}{2}-(m_e/m_i)^{1/2}$ electrons short-circuit different potential planes (perpendicular to v_1) by moving along the field lines and no positive potential rise is to be expected in the shock (Gubchenko and Zaitsev, 1979). But if the effective electron mean free path along $B(l_e^*)$ is reduced by the microturbulence, this short-circuiting probably will be reduced too as long as $l_e^*<L_s$ (see Sects. 3.2, 3.3, with $l_e^*\sim(v_{te}/\nu^*)$.

We conclude that our model calculations also give a fair estimate of the turbulence energy density in the case of quasi-perpendicular shocks defined as $\vartheta\gtrsim 50^0$, provided B_z instead of the total B is used in Sect. 2.1.

3. In order to neglect the influence of the magnetic field in the ion-acoustic instability we must have $\omega_{ce}/\omega_{pe}\ll 1$ (e.g. TK; Gary, 1979).

4. A posteriori we must check that the level W_{MS} calculated from Eq. (8) is smaller than non-linear saturation levels W_{NL} (Manheimer and Boris, 1977). We consider the following saturation mechanisms:

(i) ion-trapping resonance (Gary, 1979):

$$\frac{W}{nKT_e}\sim\frac{3}{128}\left(\frac{v_D-c_s}{v_{te}}\right)^{1/2}\left[1-4\left(\frac{T_i}{3\,T_e}\right)^{1/2}\right] \tag{9}$$

(ii) ion-resonance broadening (Caponi and Davidson, 1973):

$$\frac{W}{nKT_e}\sim\frac{3}{2\pi}\left(\frac{T_e}{T_i}\right)^{3/2}k^3\Delta k\lambda_D^4 \tag{10}$$

where Δk is the characteristic bandwidth of the excited waves.
The condition $W_{MS}<W_{NL}$ together with Eqs. (9) and (10) gives:

$$\text{(i)}\quad l<(c^2/1600\,v_A c_S)^{1/3} \tag{11}$$

$$\text{(ii)}\quad l<\frac{c}{v_A}\left(\frac{T_i}{T_e}\right)^{3/2} \tag{12}$$

where we used $v_D\sim\frac{3}{2}\,(cB/L_s 4\pi ne)$ and k, $\Delta k\sim\lambda_D^{-1}$.
With $l\sim 10$ and the ad hoc assumption that T_e and T_i do not differ too much ($T_i/T_e>0.05$), Eqs. (11) and (12) give condition 4.

Note that the conditions 4 and 1 limit the range of ω_{ce}/ω_{pe} in front of the shock considerably ($\omega_{ce}/\omega_{pe}\propto Bn^{-1/2}$ increases in the shock by a factor 2 at most).

2.3. Reflected Ions

In this paragraph we first check the existence of a beam of reflected ions, in other words how does the relaxation time of the beam compare with the crossing time ($\simeq L_s/v_1$)? Kulygin et al. (1971) studied the relaxation of a fraction (F_r) of ions moving transverse to the magnetic field. Their assumptions were: $\omega_{pi}\gg\omega_{ci}$, $F_r\gtrsim m_e/m_i$

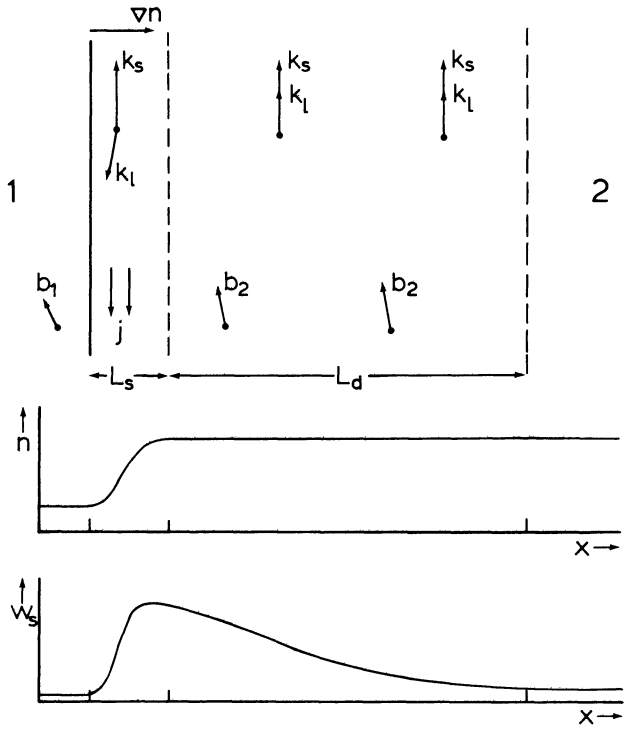

Fig. 2. Shock structure (cf. Fig. 1). The instability for ion-sound waves occurs in a thin region of thickness L_s with a current j. After their generation the ion-sound waves are convected away from the shock front and decay gradually in a region of thickness L_d. The main wave vectors of the waves are indicated in both regions (k_s for ion-sound and k_l for Langmuir waves). The direction of the main magnetic field is out of the paper; superimposed on this main field is a small component b in the plain of the paper. Also indicated are the schematic density (n) increase and the ion-sound wave energy density (W_s) across the shock

---

and velocity width $v_{tr} \gtrsim F_r^{2/5} v_{ti}$. The beam changed considerably in a time

$$t \sim 0.8 F_r^{-1} \omega_{\mathrm{LH}}^{-1}. \tag{13}$$

We thus find the relaxation time to be much larger than $\omega_{\mathrm{LH}}^{-1}$. Result (13) agrees with results of Lemons (1977) and Lemons and Gary (1978) that instabilities driven by a current perpendicular to the magnetic field have growth rates for all modes and wave vector directions both for $T_e = T_i$ and $T_e = 10\ T_i$, with an upper limit:

$$\gamma_{\max} \lesssim 0.5\ \omega_{\mathrm{LH}}. \tag{14}$$

Using a shock width $L_s \simeq lc/\omega_{pe}$ one finds the shock crossing time to be $l/(M\omega_{\mathrm{LH}})$, which in general is less than the relaxation time (13). An indirect argument from laboratory experiments is the length of the foot, a 'precursor' caused by the reflected ions (Woods, 1969, 1971; Sherwell and Cairns, 1978), with a length of order of c/ω_{pi}, which is the Larmor radius of an ion with velocity v_A: instabilities apparently are not very effective on this length scale.

Another matter is the influence of the reflected ions on the ion-acoustic instability. Including a simple distribution function of the reflected ions of the form $f_{ir} = n_r \delta(v_x - v_{xr})\, \delta(v_y - v_{yr})\, \delta(v_z)$ in Priest and Sanderson's (1972) derivation of the growth rate, we just find an extra numerical factor

$$\frac{n_e}{[n_i + n_{ir}(1 - v_{yr}k_y/\omega)^{-3}]}. \tag{15}$$

Our marginal stability calculations, using $\gamma = 0$, are unaffected by the reflected ions. Note that the equality $1 - v_{yr}k_y/\omega = 0$ cannot be satisfied since $v_{yr} \gtrsim v_A$ (see below), $\omega/k_y \sim c_s$ and $v_A > c_s$ and therefore does not lead to a new solution.

The last point we should like to mention is the terminal velocity of the beam. Woods (1969) and Sherwell and Cairns (1977) after extensive calculations give beam velocities of order v_1. This result also follows roughly from an argument using the current and ∇T-drift as calculated by Priest and Sanderson (1972), assuming the variation in temperature and density to have the same scale. Gubchenko and Zaitsev (1979) on the contrary claim an increase in kinetic energy by a factor m_i/m_e. The basic flaw in the argument of these authors appears to be the neglect of the kinetic energy in the x-direction in their Eq. (24). It is very doubtful whether the calculations of Gubchenko and Zaitsev, in which they find $v_y \gg v_1$, are valid since they do not calculate v_y at the instant that $v_x \simeq v_1$, when the particle crosses the front.

3. Radio Emission from a Collisionless (Quasi-) Perpendicular Shock

3.1. Estimates of the Radio Emission

Morse and Greenstadt (1976) successfully used the marginal stability method of Manheimer and Boris (1972) to calculate the structure of the Earth's bow shock. In this section we will put some general constraints on the radio emission from a collisionless shock.

In Sect. 2.1. we estimated the turbulence energy density W_s and the shock thickness L_s. If the shock structure is determined by the ion-acoustic turbulence electromagnetic radiation from the shock can only be expected if high-frequency plasma waves and/or fast electrons are produced. Since ion-acoustic waves only heat and do not accelerate (Kaplan et al., 1974), we consider the production of high-frequency plasma waves from the low-frequency turbulence. Langmuir waves are produced by the turbulent Bremsstrahlung mechanism (Tsytovich et al., 1975; Kuijpers, 1980a, b). In this process electrons that are in resonance with ion-sound waves ($\omega_s = k_s \cdot v$ where ω_s is the ion-sound wave frequency, k_s its wave vector and v the particle velocity) are accelerated. Thus they radiate in all possible wave modes, in particular Langmuir waves. We assume that the ion-sound spectrum is confined to a cone around the electron drift direction as is observed in the laboratory (Stenzel, 1978). Then for a stationary shock the spatial distribution of ion-sound waves consists of two regions as indicated in Fig. 2: a thin region of thickness lc/ω_{pe} with the ion-sound wave level of Eq. (8) and a larger region with a thickness (neglecting ion-sound propagation)

$$L_d \simeq \tfrac{1}{4} M v_{A_1} t_d \tag{16}$$

without a current where the ion-sound waves are left behind by the shock front and decay on a time scale t_d determined by a combination of collision and Landau damping and where we have assumed a strong adiabatic shock wave ($v_2 \simeq v_1/4$).

In both regions Langmuir waves are produced by turbulent Bremsstrahlung be it under different conditions.

In the thin shock front proper (see Fig. 2) where the electric current is present, upconversion only proceeds in directions anti-

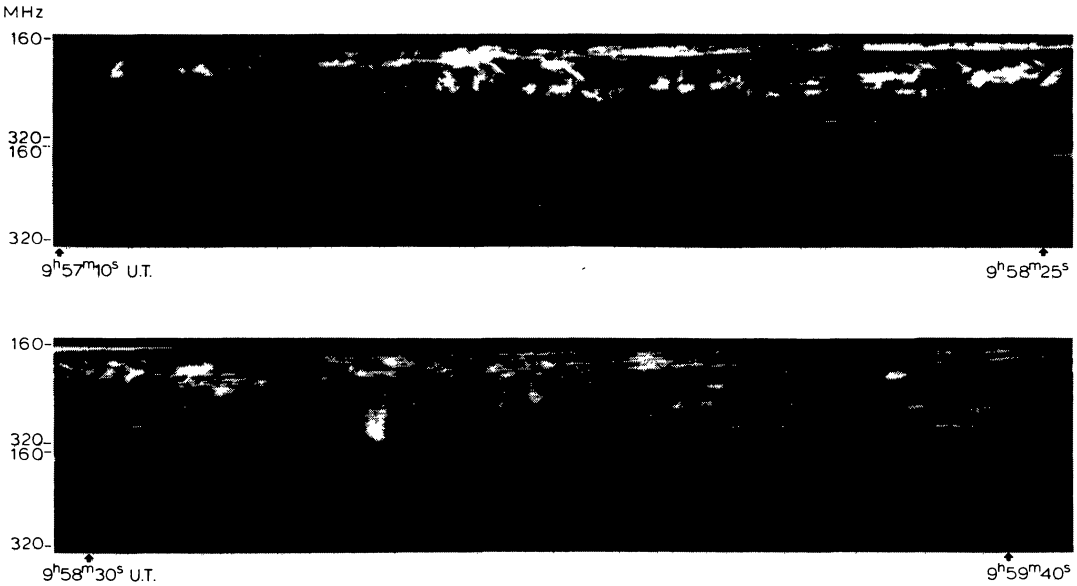

Fig. 3. Dynamic radio spectrogram of a type II radio burst observed with the 60-channel spectrograph (at present at Dwingeloo) on 5 June 1969. The lower half of each picture shows the flux recordings (range 40 dB over quiet sun level ($\simeq 1$–$2\ 10^{-21}$ W m^{-2} Hz^{-1}); time constant 0.02 s); the upper half of each picture shows the flux variations with respect to a floating zero level (averaging time constant 3 sec; sensitivity 0.2 dB; dynamic range ± 1.7 dB). The 60 channels are evenly spaced in the interval 160–320 MHz (separation of 2.7 MHz) and each has a bandwidth of 0.9 MHz. The time interval between two ticks is one second. The observed emission originates from a shock wave travelling through the solar corona; because of the relatively small drift rate (-0.7 MHz s^{-1}) the emission occurs presumably at the fundamental of the electron plasma-frequency

parallel to the ion-sound waves and most efficiently for (Kuijpers, 1980a, b)

$$k_l \ll k_D \ll k_s. \tag{17}$$

Here k_l is the wave number of the Langmuir waves, k_s the wave number of the ion-sound waves and $k_D = \omega_{pe}/v_{te}$ is the Debye wave number. Further substantial upconversion proceeds only for those Langmuir waves which are comoving with the shock front for a sufficient number of e-folding periods that is for directions ϑ_l with respect to the shock normal for which

$$\frac{L_s \gamma_l}{v_g \cos\vartheta_l - M v_A} \gg 1. \tag{18}$$

Here v_g is the group velocity of the Langmuir waves and the turbulent Bremsstrahlungs rate is

$$\gamma_l \simeq \omega_{pe} \frac{v_D}{v_{te}} \frac{k_l}{k_s} \frac{W^s}{nKT_e} \simeq l \frac{k_l}{k_s}\left(\frac{2}{\beta}\right)^{1/2} \frac{c_s^2}{v_{te}} \frac{\omega_{pe}}{c}, \tag{19}$$

where we have used a drift velocity $v_D \simeq c_s$, a stationary ion-sound level as given by Eq. (8) and a front thickness $L_s = lc/\omega_{pe}$. Substituting Eq. (19) into Eq. (18) and putting $v_g \simeq v_{te}$ we find with Eq. (17):

$$\cos\vartheta_l - M \frac{v_A}{v_{te}} \ll l^2 \frac{m_e}{m_i} \frac{k_l}{k_s}\left(\frac{2}{\beta}\right)^{1/2} \ll 1. \tag{20}$$

Therefore only the Langmuir waves within a narrow cone with projected group velocities nearly equal in magnitude to the shock speed and in a direction opposite to the fluid motion are amplified.

In the region behind the thin shock front (see Fig. 2) Langmuir waves are produced in the absence of a current due to the anisotropy of the ion-sound spectrum. In this case the wave vectors of the Langmuir waves are parallel to those of the ion-sound waves with a growth rate (19). A backward travelling Langmuir wave stays in the amplifying region for a number of e-folding periods equal to [see Eqs. (16) and (19)]

$$4M \frac{V_{A1}}{c}\left(\frac{T_i}{T_e}\right)^{1/2} \frac{k_l}{k_s}\left(\frac{2}{\beta}\right)^{1/2}\left(\frac{m_e}{m_i}\right)^{1/2} N_D, \tag{21}$$

where we have used a value of v_{te} for the group velocity of the Langmuir waves, $l \simeq 10$ and the collisional damping rate of ion-sound for t_d (Kaplan and Tsytovich, 1973)

$$t_d \simeq \frac{1}{0.6}\left(\frac{T_i}{T_e}\right)^{1/2} \frac{N_D}{\omega_{pi}}. \tag{22}$$

Clearly expression (21) is much larger than unity in the solar corona.

Thus we conclude that the Langmuir waves are generated in roughly two antiparallel directions and at different background densities. We expect that Landau damping will create streams of suprathermal electrons in both directions along the magnetic field. Due to propagation these accelerated electrons become unstable away from their source regions where they create secondary Langmuir waves.

3.2. Type II Radiobursts of the Sun

Type II radiobursts (Wild and Smerd, 1972) are associated with flares. The standard theory of the phenomenon uses a weak shock in the collisionless plasma of the corona (Rosenberg, 1976), with

Table 1. Parameters of a type II radio burst of the Sun (gaussian cgs units)

n_e	$\simeq 5\ 10^8\ \mathrm{cm}^{-3}$	$\omega_{pe}/2\pi$	$\simeq 8.98\ 10^7\ n_8^{1/2}$ Hz
T_e	$\simeq 10^6$ K	$\omega_{ce}/2\pi$	$\simeq 2.80\ 10^6\ B$ Hz
B	$\simeq 6$ G	v_{te}	$\simeq 3.89\ 10^8\ T_6^{1/2}$ cm s^{-1}
v_1	$\simeq 10^3$ km s^{-1}	v_A	$\simeq 1.86\ 10^7\ B\ n_8^{-1/2}$ cm s^{-1}
Size	$\simeq 1\ R_\odot^2$	c_s	$\simeq 9.08\ 10^6\ T_6^{1/2}$ cm s^{-1}
Radio: S_f	$\simeq 100$ s.f.u. (10^{-17} erg cm^{-2} Hz^{-1} s^{-1})	λ_D	$\simeq 6.90\ 10^{-1}\ T_6^{1/2}\ n_8^{-1/2}$ cm
f	$\simeq 200$ MHz	N_D	$\simeq 3.28\ 10^7\ T_6^{3/2}\ n_8^{-1/2}$
Δf	$\simeq 5$ MHz	β	$\simeq 3.47\ 10^{-1}\ T_6\ n_8\ B^{-2}$
Duration	$\simeq 5$ min		

References: Wild and Smerd, 1972; Dulk and McLean, 1978; Dulk, 1980

as a popular version the perpendicular ($v \perp B$) shock. In Sect. 2.3. we criticized Gubchenko and Zaitsev's (1979) mechanism to accelerate protons, which are observed to be associated with type II bursts (cf. Achterberg and Norman, 1980).

We shall now apply the above results concerning the structure of perpendicular collisonless shocks to explain type II radio bursts. Concerning the perpendicular nature of the type II shock indeed the model by van Tend and Kuperus (1978) naturally gives rise to outward motion perpendicular to the above magnetic fields (e.g. their Figs. 1 and 5).

As in other kinds of solar radio bursts the Langmuir waves are expected to give rise to electromagnetic radiation at the fundamental and possibly at the second harmonic of the plasma frequency. From the foregoing a dynamic radio spectrum as observed with the Utrecht 60-channel spectrograph (Fig. 3) can be understood. The total flux measurements (lower group of channels) show two parallel drifting emission bands. The floating zero flux recordings (upper group of channels) show a wealth of fine structures. Mainly they consist of bursts with relatively fast positive and negative drift rates with the positive drift bursts starting from the low frequency emission band and the negative drift bursts starting from the higher frequency emission band. In our shock wave structure (see Fig. 2) the slowly drifting bands would correspond to (either fundamental or second harmonic) emission resulting from the excited Langmuir waves in the thin shock front (the lower frequency band) and from Langmuir waves excited in the more extended region behind the front (the higher frequency band). In each region acceleration of electrons is expected to take place along the magnetic field direction in which the Langmuir wave distribution is peaked. If the magnetic field has a small component b in the plane of Fig. 2 these accelerated electrons would lead to secondary plasma radiation extending with positive drift rate from the lower frequency band and with negative drift rate from the higher frequency band as is observed in Fig. 3.

The discrete nature of the fast drift bursts can be understood from the prey-predator behaviour of ion-sound and Langmuir waves if the turbulent Bremsstrahlung mechanism is operating. The evolution of the combined system of Langmuir and ion-sound waves in the shock can be modelled by Volterra-Lotka equations (Kuijpers, 1978).

Thus in principle short pulses of electrons and of radiation spikes are expected to be produced.

We shall now discuss the observed brightness temperature and flux in relation with the predictions of our model.

Table 1 gives typical values of some relevant qualities and the resulting plasma parameters. We shall assume a magnetic field strength of 6 G and a Mach number $M \sim 2$. For l we use a modest value 7. From the model discussed in Sect. 2.1., the conditions mentioned in Sect. 2.2. being fulfilled, we have

$$L_s \sim \frac{7c}{\omega_{pe}} \tag{23}$$

$$W_s \sim 2.7\ 10^{-5}\ n_8^{1/2} T_6 B \text{ erg cm}^{-3} \tag{24}$$

A typical (isotropic) luminosity of type II radio bursts is

$$\mathscr{L}^R \sim 1.3\ 10^{17} \text{ erg s}^{-1}. \tag{25}$$

Further for the extent of a typical type II burst we take a circular area of one square solar radius. Then the observed flux can be expressed as

$$S_f = 2\pi K T_b r_\odot^2 f^2 c^{-2}, \tag{26}$$

where $r_\odot$ denotes the solar radius expressed in units of 1 AU. Then we have a brightness temperature of

$$T_b^R \sim 5.4\ 10^8 \text{ K} \tag{27}$$

with index 'R' denoting an observed (radio) quantity.

The observed brightness temperature provides an estimate of the minimum required brightness temperature of the Langmuir waves and therefore of the ion-acoustic waves:

$$T_b^s \simeq \frac{W_s}{K} k_D^{-3} (2\pi)^3 \simeq \frac{l v_A}{c} n T k_D^{-3} (2\pi)^3 = 56\pi^3 \frac{v_A}{c} N_D T \tag{28}$$

Clearly this theoretical upper limit is much larger than the observed brightness temperature Eq. (27) for coronal temperatures.

We now compare the estimated production rate of Langmuir waves in the shock with the observed electromagnetic flux. Using a transverse shock dimension $D = 1\ R_\odot^2$ we find the total production rate of Langmuir waves with Eqs. (16), (22), (19) and Table 1 to be

$$\begin{aligned}\mathscr{L}^l &\simeq \gamma_l D L_d W^l \\ &= \frac{l}{2.4} \frac{k_l}{k_s} \left(\frac{2}{\beta}\right)^{1/2} \frac{v_{ti}}{c} D M v_{A_1} n K T_e \left(\frac{W^l N_D}{n K T_e}\right) \\ &= 8.2\ 10^{27} \left(\frac{T_i}{T_e}\right)^{1/2} \frac{W^l N_D}{n K T_e} \text{ erg s}^{-1}\end{aligned} \tag{29}$$

for $l = 7$, $k_l/k_s = 1$. Since the Langmuir wave energy density is much larger than the thermal noise level (of order nKT_e/N_D) the Langmuir luminosity (29) is much larger than the observed electromagnetic luminosity (25).

Finally the Langmuir wave luminosity cannot be larger than the ion-acoustic wave luminosity

$$\begin{aligned}\mathscr{L}_s &\simeq \tfrac{1}{4} M v_{A_1} D W^s \\ &= 4.9\ 10^{25} \text{ erg s}^{-1}\end{aligned} \tag{30}$$

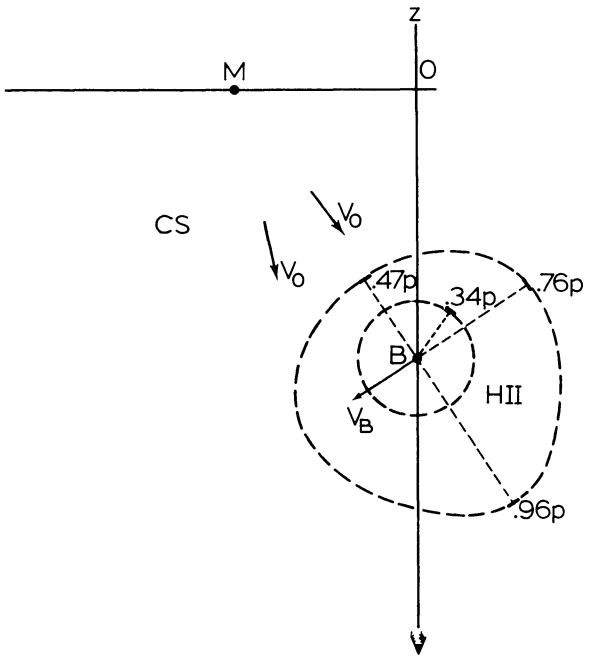

Fig. 4. Geometry of the Antares (α Sco) system from van der Hucht et al. (1980). Wade and Hjellming's (1971b) radio beam with radius 0.34 p and the H II region as calculated by Van der Hucht et al. are indicated. $M0 \equiv p = 2''9 = 522$ AU; the velocity of the circumstellar shell (CS) $v_0 = 17$ km s^{-1}; the orbital velocity of the B star $v_B = \pm 4$ km s^{-1} (we neglect this velocity); $-p \leqq$ B0 $\leqq -2$p, we take B0 $= -1.5$ p

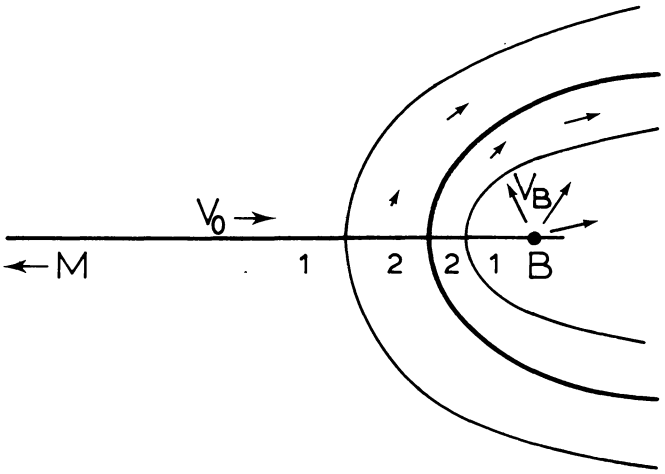

Fig. 5. Schematic picture of the double shock system in the winds from the M star (wind velocity v_0) and from the B star (wind velocity v_B). The regions ahead of the respective shock is indicated by 1, the region behind the shock by 2. The shocked winds are separated by a contact discontinuity (heavy line)

for the same conditions as before. Clearly estimate (30) is more restrictive on the Langmuir luminosity than estimate (29). At the same time it is clear from the estimate (29) (in which no back reaction into sound waves is included) that the turbulent bremsstrahlung is a very efficient process.

For a perpendicular shock the ratio of the electron mean free path (the electron gyro radius) to the shock thickness can be written as

$$\frac{1}{l}\left(\frac{\beta}{2}\right)^{1/2}, \tag{31}$$

which indeed is much smaller than unity as required for a collisionless shock. Further the ratio of the effective electron mean free path along the field [see Eq. (4)] to the shock thickness is

$$\frac{l_e^*}{L_s} \simeq \frac{v_{te}\omega_{pe}}{\nu^* lc} = \frac{v_{te}}{l^2 v_A} \lesssim 1 \tag{32}$$

in the corona. Thus a strictly perpendicular configuration probably is not required.

We conclude that the observed luminosity, brightness temperature and fine structures in type II solar radio bursts can be explained as originating from the ion-acoustic turbulence of a quasi-perpendicular collisionless shock.

Table 2. Parameters of the Antares (α Sco) system (van der Hucht et al., 1980)

	α^1 Sco	α^2 Sco
Spectral type	M 1.5 Iab	B 2.5 V
Radius $R/R_\odot$	810	4.6
Luminosity log $(L/L_\odot)$	4.7	3.3
Temperature $T_{\rm eff}$ (K)	3500	18 500
Mass $M/M_\odot$	23	8.5
Distance	180 pc	
Projected separation	$p = 2''9$ ($\triangleq 522$ AU)	

3.3. Radio Emission from Antares B: a Shock?

3.3.1. Description of the System

In the Antares (α Sco) system a red supergiant (M 1.5 Iab) has a strong mass loss, resulting in a circumstellar shell (CS), through which plows a companion star (B) (see Fig. 4). In this section we adopt the model by van der Hucht et al. (1980), based on UV observations of circumstellar lines formed between the featureless continuum of the fast rotating B star and the observer. The expansion velocity of the CS is quite constant spatially (Bernat, 1977). The radiation of the B star ionizes locally the CS matter, Fe II emission lines are observed (Swings and Preston, 1978). Some relevant parameters of the system and physical conditions of the shell are indicated in Table 2 and Table 4, first column. Note that the low electron temperature quoted was measured in different lines and must be explained by NLTE (van der Hucht et al., 1980).

Kudritzki and Reimers' (1978) derivation of the ionizing shock between the H II region around the B star and the neutral CS matter, with van der Hucht's parameters, gives a weak ionizing shock at a distance of 610 AU from M (cf. van der Hucht's 695 AU). Since the shock is weak, we conclude that the expansion velocity of the shell changes very little in the H II region.

3.3.2. Radio Observations

Radio binary stars (Hjellming, 1974) have a variable emission, both in intensity and spectrum. They appear to be a rare stellar activity, but the system we consider here (with a longer period than

the other radio binaries) is certainly unique. Wade and Hjellming (1971a, b) first detected cm-radiation from the B star (beam diameter 2″); recently this has been confirmed by Olnon (personal communication) and by Gibson (1978; 1″ beam). According to Hjellming and Gibson (1979) the emission region is located between M and B, just off B, and they conclude that probably a bow shock around the companion star is generating the observed radio emission. We list the observations (see also Wendker, 1978) in Table 3:

Table 3. Radio emission from α Sco

	Wavelength (cm)	Flux (mfu)
Olnon (in August, September 1977)	21	5.5
Gibson (1978)	21	9
Gibson (1978)	6	3
Wade and Hjellming (1971a)	11.1	5–8
Wade and Hjellming (1971b)	3.7	10 (flare)

Note the apparent non-thermal spectrum which cannot be explained from a HII region.

Gibson (1978) concludes that the radio emission of Antares B appears to be quite stable over several years; he also observed a flare of the M giant with a radio luminosity $\mathscr{L} \sim 5\ 10^{26}$ erg s^{-1} (with $\Delta f \sim f = 5$ GHz), somewhat larger than the radio output of a solar flare.

Assuming a constant spectrum of 5 mfu over $\Delta f \sim 10^{10}$ Hz and a distance of 180 pc we find a minimum steady radio luminosity of

$$\mathscr{L}^R = 1.8\ 10^{27} \text{ erg s}^{-1}. \tag{33}$$

3.3.3. Shocks

Apart from the ionization shock (see 3.3.1.) shocks can arise in the Antares system in three ways: if the B star has no wind the stellar wind from the M star will be enhanced near the companion due to accretion and an accretion shock forms; alternatively if also the B star has a wind the two winds collide supersonically and give rise to a system of two shocks separated by a contact discontinuity (see also Kudritzki and Reimers, 1978). Finally the presence of a magnetosphere around the B star would lead to a bow shock.

B stars are known to possess stellar winds (Cassinelli et al., 1978). Moreover we shall show that the first possibility, of an accretion shock in the absence of a B wind, is incompatible with the X-ray observations. Finally we shall prove that a bow shock around a magnetosphere cannot explain the observed radio emission.

3.3.4. Accretion

The B star is embedded in a stellar wind from the M 1.5 Iab star with a hydrogen atom density

$$n_{\mathrm{H}}^M \simeq 4.6\ 10^4\ r^{-2} \text{ cm}^{-3}, \tag{34}$$

where r is the distance from the M star in units of the distance between M and B star which we have put equal to $(3.25)^{1/2}\,p$. (van der Hucht et al., 1980). The wind velocity is $v_0 \simeq 17$ km s^{-1}. Due to infall the final velocity of this matter at the surface of the B star would be

$$v_{\mathrm{esc}} \simeq \left(\frac{2GM_B}{R_B}\right)^{1/2} (1-\Gamma)^{1/2} \simeq 611 \text{ km s}^{-1}, \tag{35}$$

where $\Gamma = 2.53\ 10^{-5}\ \frac{L_B}{L_\odot}\ \frac{M_B}{M_\odot}$ is the correction due to radiation pressure (Abbott, 1978). Therefore the accreted gas will reach a temperature

$$T_a \simeq \frac{m_{\mathrm{H}} v_{\mathrm{esc}}^2}{2\left(2X + \frac{3}{4}Y\right)K} \simeq 1.4\ 10^7 \text{ K}, \tag{36}$$

where $X \simeq 0.73$ is the weight fraction of hydrogen and $Y \simeq 0.25$ that of helium. Thus the gas would be emitting soft X-rays.

The rate of accretion is in between the geometrical accretion rate

$$\dot{M} \simeq \pi R_B^2 \varrho_M v_0 \simeq 6.68\ 10^{-16}\ M_\odot \text{ yr}^{-1} \tag{37a}$$

and the Hoyle-Littleton rate

$$\dot{M} \simeq \pi R_a^2 \varrho_M v_0 \simeq 3.97\ 10^{-9}\ M_\odot \text{ yr}^{-1}, \tag{37b}$$

where the radius of gravitational attraction is given by

$$R_a = \frac{2GM_{\mathrm{B}}}{v_0^2} \simeq 2.4\ 10^3\ R_{\mathrm{B}}. \tag{38}$$

If the energy of infall is radiated in X-rays, the luminosity due to accretion would be

$$\mathscr{L}_{\mathrm{X}} = \dot{M} v_{\mathrm{esc}}^2 \simeq 1.59 \times 10^{26} - 9.43\ 10^{32} \text{ erg s}^{-1}, \tag{39}$$

depending on the chosen accretion rate (37a) or (37b).

At present no X-rays (0.2–3 keV) have been observed from the Antares system by the Einstein satellite with an upper limit of (Vaiana et al., 1980)

$$\mathscr{L}_{\mathrm{X}}^{\mathrm{obs}} < 2\ 10^{29} \text{ erg s}^{-1}. \tag{40}$$

The actual rate of accretion will be close to the limit (39b) since the orbital velocities of the stars are only a few kilometers per second. Thus the observations contradict strong gravitational accretion. This accretion will not occur if the B-star is surrounded by a magnetosphere or alternatively if the B-star itself has a sufficiently strong wind, which cases we shall consider now.

3.3.5. Bow Shock

If the B star is surrounded by a magnetosphere, a bow shock would occur in the stellar wind from the M star. We give an upper limit for the radio luminosity from such a shock applying the model of a perpendicular collisionless shock.

To have $\beta \lesssim 1$ in CS, the minimum magnetic field strength required is $B_{cr} = 3\ 10^{-4}$ G (see Table 4). This field is much stronger than a typical interstellar field and should originate in the M star. For a Parker stellar wind ($B_r \propto r^{-2}$) the radial field at the surface of the M star should then be $B_r\,(R_M = 3.8 \text{ AU}) \gtrsim 18.4$ G assuming a distance of 941 AU between the M star and the magnetosphere. Numerical calculations by Johnson (1974, e.g. his K1 model) show that deep in the convection zone such fields have an energy density less than that of the thermal gas, as required by a dynamo mechanism. As long as $\beta \leqq 1$ the precise value of the magnetic field is not critical to our results (provided of course that $v_{A_1} < v_1$). The conditions of Sect. 2.2 are met assuming that the CS magnetic field spirals outward as in the Parker solar wind. Similar to the argument of Eq. 30 we find that the radio luminosity

Table 4. Physical conditions in the double shock system

	M-wind		B-wind	
	1 (pre-shock)	2 (post-shock)	2 (post-shock)	1 (pre-shock)
n_H (cm^{-3})	$5.4\ 10^4$	$2.1\ 10^5$	19	4.8
T_e(K)	500	$1.6\ 10^4$	$1.8\ 10^8$	10^5
v_A (km s^{-1})	2.8[a]	5.7[a]	$< 5.1\ 10^3$	$< 2.5\ 10^3$
$\omega_{pe}/2\pi$ (Hz)	$2.2\ 10^6$	$4.5\ 10^6$	$4.3\ 10^4$	$2.1\ 10^4$
$\omega_{ce}/2\pi$ (Hz)	$8.4\ 10^2$	$3.4\ 10^3$	$3.4\ 10^4$	$8.4\ 10^3$
v_{te} (km s^{-1})	87	$4.9\ 10^2$	$5.2\ 10^4$	$1.2\ 10^3$
λ_D (cm)	0.62	1.7	$1.9\ 10^4$	$9.2\ 10^2$
N_D	$1.7\ 10^4$	$1.6\ 10^6$	$1.9\ 10^{14}$	$5.2\ 10^9$

[a] See Sect. 3.3.5.

cannot exceed

$$\mathscr{L}^R < \tfrac{1}{4} M v_{A_1} D W^s \simeq 1.7\ 10^{18}\ D/\pi R_B^2 \text{ erg s}^{-1}. \quad (41)$$

Here we have used Eq. (8), Table 4, $M=2$, $l=7$, strong adiabatic shock relations and we have estimated the physical quantities in the shock front to be half their maximum values behind the front. To be consistent with the observed radio luminosity (33) the transverse shock surface should be more than 10^9 times the projected B-star surface. This is ruled out by the observations: compare the required size of 1400 AU with Wade and Hjellming's (1971b) 340 AU beam diameter.

Moreover the observed radio luminosity (33) corresponds to the total wind energy flow through a circular area with radius more than one hundred B-stellar radii.

Thus we conclude that a magnetosphere with a surrounding bow shock can be ruled out as the origin of the observed radio emission.

3.3.6. Two Colliding Winds

A simple estimate for the mass loss rate of the B star can be obtained from the radiation pressure in one strong line (Lucy and Solomon, 1970)

$$-\dot{M} \simeq \frac{\pi}{c} 4\pi R_B^2 \frac{F_c}{\lambda}, \quad (42)$$

where F_c is the continuum flux and λ the wavelength of the absorbing line. Using $T_{\text{eff}}=18\,500$ K at $\lambda \simeq 1000$ Å we have $F_c \simeq 9.52\ 10^{-4}$ erg cm^{-2} s^{-1} Hz^{-1} and

$$-\dot{M}_B \simeq 2.04\ 10^{-10}\ M_\odot \text{yr}^{-1}. \quad (43)$$

The rate of mass loss of main sequence stars is badly known from the observations (e.g. Cassinelli et al., 1978). Especially in the range $1.5\ 10^3 < L/L_\odot < 3\ 10^4$ (note that $L_B/L_\odot \simeq 2.2\ 10^3$) the rate of mass loss depends strongly on the rotational velocity of the star so that appreciable mass loss occurs as soon as $v_{\text{rot}} \gtrsim 200$ km s^{-1} (Furenlid and Young, 1980; cf. Snow and Marlborough, 1976). In our case $v_{\text{rot}}^B \sin i \simeq 250$ km s^{-1} (Kudritzki and Reimers, 1978) and therefore we expect the B star to have a stellar wind. We estimate its mass loss by scaling the mass-loss rate of the early main sequence star τ Sco (B0 V) (Lamers and Rogerson, 1978):

$$-\dot{M}_B \simeq 7.0\ 10^{-9} \frac{L_B}{L_{\tau\,\text{Sco}}} M_\odot \text{yr}^{-1} \simeq 4.26\ 10^{-10} M_\odot \text{yr}^{-1}, \quad (44)$$

of the same order as the simple estimate (42). We note that this star does not show appreciable rotation; hence in our case Eq. (44) represents a lower limit to the actual mass loss.

Further we assume the final velocity of the radiation driven wind to be (Abbott, 1978)

$$v_B \simeq 3 v_{\text{esc}} \simeq 1800 \text{ km s}^{-1}, \quad (45)$$

which is expected to be reached at a distance of 10–30 R_B (Cassinelli et al., 1978). Further for the temperature of this wind we shall use the commonly adopted value of τ Sco (B0 V)

$$T_B \simeq 10^5 \text{ K}. \quad (46)$$

In this case the stellar wind from the M star collides with the wind of the B star; in the corotating frame of both stars a stationary system of two shock waves is set up, separated by a contact discontinuity (see Fig. 5). The location of the contact discontinuity along the line from B to M can be found by equating the dynamic pressures of both winds

$$n_H^B v_B^2 = n_H^M v_0^2, \quad (47)$$

where

$$n_H^B = -\frac{\dot{M}_B}{1.37\ m_H\ 4\pi r_B^2 R_B^2 v_B} \simeq 5\ 10^7 r_B^{-2} \text{ cm}^{-3} \quad (48)$$

and r_B is the distance from the center of the B star in units of R_B. Then from Eqs. (48), (47), (45) and (34) we find

$$r_B \simeq 3.2\ 10^3. \quad (49)$$

Again we assume that the shocks are strong and adiabatic so that the post-shock densities and transverse magnetic fields are four times the pre-shock values and the temperatures of the shocked gas can be found by equating the shocked gas pressure to $\frac{3}{4}$ the pre-shock dynamic pressure. The physical conditions in the various regions are assembled in Table 4.

An upper limit for the magnetic field in the B wind can be found by requiring the magnetic pressure to be less than the dynamic pressure.

Thus we find for the unshocked field

$$B_1 < 3.0\ 10^{-3} \text{ G}. \quad (50)$$

The corresponding pre- and post-shock Alfvén speeds are given in Table 4. From the Table it can be seen that the observed radio emission at a frequency $f_0 = 8.1\ 10^9$ Hz cannot be explained as the direct result of the excitation of plasma waves in the shock system. Rather accelerated electrons are required with typical Lorentz factors of order

$$\gamma \simeq \left(\frac{2\pi f_0}{\omega_{pe}}\right)^{1/2} \quad \text{or} \quad \left(\frac{2\pi f_0}{\omega_{ce}}\right)^{1/2} \approx 100 \quad (51)$$

depending on the radiation mechanism (inverse Compton scattering on the Langmuir waves or synchrotron radiation).

Table 4 shows that the Debye number ($N_D \equiv n_e \lambda_D^3$) is extremely large in the post-shock B-wind. Thus collective plasma phenomena are very important in this region; for instance the collisional damping length of Langmuir waves is extremely large in this region, of order $N_D \lambda_D \simeq 2.5\ 10^5$ AU. Therefore we take the shocked B-wind region to be the site of the acceleration of electrons and of the observed radio emission. Again using the argument of Eq. (30)

we find that the radio luminosity cannot exceed [see also Eq. (41)]:

$$\mathscr{L}^R < 1.8\ 10^{30}\ \frac{D}{\pi r_B^2}, \tag{52}$$

where we have used $M=2$, $v_A=v_{A_1}=900$ km s^{-1}, $l=7$, values for n and T_e from the third column of Table 4 and r_B as given by Eq. (49). Evidently the observed radio emission is less than one per mille of the ion-sound luminosity, which again points to the shocked B-wind region as the site of radio emission.

We conclude that the observed stationary radio emission from the Antares B companion can be explained energetically by a shock which is formed when a wind of the B star clashes with the circumstellar wind of the M star. However, the radio emission cannot be explained directly as radiation at the electron plasma frequency. Rather acceleration of energetic electrons with $\gamma \approx 100$ should take place in the shock front.

4. Conclusions

We have estimated the ion-acoustic wave energy density in collisionless perpendicular shocks using the hypotheses of marginal stability and (for large Mach numbers) ion heating behind the shock from the decay of the beam of reflected ions. The region of microturbulence in the shock consists of two parts: a thin sheet of thickness $\simeq 10c/\omega_{pe}$, where the ion-sound waves are excited, and a larger region of thickness $\lesssim \frac{1}{4} MN_D v_{A_1}/\omega_{pi}$, where the excited ion-sound waves are damped.

High-frequency Langmuir waves are generated from the ion-acoustic turbulence through turbulent Bremsstrahlung. In the case of solar type II bursts this mechanism can explain the observed radio emission and the observed fine structures.

In the case of the Antares system probably a double shock system is formed where the observed circumstellar M wind hits the expected wind of the B star ("Du choc des deux armées, la nature est encore agitée tout autour". A Daudet). Because of the large Debye number in the shocked B wind, the latter shock has a powerful turbulent wave energy density which is energetically sufficient to account for the observed radio emission. However, Langmuir waves in the shock cannot explain the observed high-frequency radio emission and wave acceleration of electrons is required. We predict that the site of the radio emission is located at a projected distance 0.″17 ahead of the B star in the direction of the M star.

Feldman (see also Feldman and Kwok, 1979) informed us that measurements by Gibson with the VLA show the steady non-thermal radio source of Antares to be located in between the M and B star at a projected distance of 0.″65 from B. This would imply that the mass loss of B is a factor ~ 15 larger than our estimate in section 3.3.6. where we neglected a probable enhancement of the mass loss due to rotation.

Alternatively, the above interpretation of the location of radio emission would constitute a possibility to measure indirectly small mass losses which would otherwise be unobservable.

Such a mass loss ($\sim 6\ 10^{-9}\ M_\odot$ yr^{-1}) compares well with recent data in Lamers (1981). Moreover, in the above estimates we have assumed a spherically symmetric wind.

Acknowledgements. We gratefully acknowledge discussions or correspondence with Drs. A. Achterberg, R. A. Cairns, P. A. Feldman, H. F. Henrichs, K. A. van der Hucht, S. Kwok, D. S. Lemons, C. Slottje and F. Verbunt. We appreciate the referee's comments. Finally, we thank Mrs. H. Tappermann for typing the manuscript, Mr. E. Landré for making the figures and Mr. B. Kramer for providing the picture of the type II radio burst.

Most Important Symbols

B	magnetic field strength
β	$\equiv nKT_e/(B^2/8\pi)$
γ	growth rate
c_s	sound velocity $(KT_e/\mathrm{m}_i)^{1/2}$
D	transverse shock dimension
e	electron charge (absolute value)
f	frequency
f_j	distribution function of component j
F_r	fraction of reflected ions
k	wave vector
K	Boltzmann constant
λ_D	$\equiv k_D^{-1}$ Debye length
L_d	thickness of region of decaying ion-sound waves
L_s	shock thickness
$\mathscr{L}$	luminosity
l	$=L_s\omega_{pe_1}/c$
l_e^*	effective electron free path
m_j	particle mass of type j
M_A	Mach number relative to v_{A_1}
M	Mach number relative to magneto-acoustic velocity
ν^*	effective collision frequency
n	electron density
n_H	hydrogen atom density
ω	angular wave frequency
ω_{pj}	plasma frequency of j
ω_{cj}	gyrofrequency of j
ω_LH	lower hybrid frequency $(\omega_{ce}\omega_{ci})^{1/2}$
p	522 AU in the Antares system (see caption Fig. 4)
r_{Lj}	Larmor radius of component j (usually $r_{Lj}\equiv v_{tj}/\omega_{cj}$)
S_f	flux at frequency f
S_j	degrees of freedom of component j
T_j	temperature of component j
ϑ	angle between B_1 and v_1
t_c	collision time
t_d	damping time of ion-sound waves
v_D	drift velocity
v_{tj}	thermal velocity of component j
v_A	Alfvén velocity
W	turbulence energy density
Δ ( )	jump across shock

Subscripts$_{1,2}$ indicate conditions well before and, respectively, well after the shock front.

Suffix r: reflected

s: shock / ion-sound wave

l: Langmuir wave

Sub- or superscript M: M star

B: B star

References

Abbott, D.C.: 1978, *Astrophys. J.* **225**, 893

Achterberg, A., Norman, C.: 1980, *Astron. Astrophys.* **89**, 353

Bernat, A.P.: 1977, *Astrophys. J.* **213**, 756

Biskamp, D.: 1973, *Nuclear Fusion* **13**, 719
Cairns, R.A.: 1980, Symp. Earth Bow Shock 1978, Strassbourgh (in press)
Caponi, M.Z., Davidson, R.C.: 1973, *Phys. Rev. Letters* **31**, 86
Cassinelli, J.P., Castor, J.I., Lamers, H.J.G.L.M.: 1978, *Proc. Astron. Soc. Pacific* **90**, 496
Dulk, G.A.: 1980, in Radiophysics of the Sun, IAU *Symp.* No. 86, M. R. Kundu and T. E. Gergeley (eds.), p. 419
Dulk, G.A., McLean, D.J.: 1978, *Solar Phys.* **57**, 279
Feldman, P.A., Kwok, S.: 1979, *J. Roy. Astron. Soc. Can.* **73**, 271
Formisano, V.: 1977, *J. de Phys.* **38** C6–65
Furenlid, I., Young, A.: 1980, *Astrophys. J.* **240**, L59
Galeev, A.A.: 1976, in *Physics of Solar and Planetary Environments*, ed. D. J. Williams, American Geophysical Union, pp. 464–466, p. 487
Gary, S.P.: 1979, to publ. Nuclear Fusion (preprint LA-UR-79-682)
Gibson, D.M.: 1978, *Bull. Amer. Astron. Soc.* **10**, 631
Greenstadt, E.W., Fredricks, R.W.: 1979, in *Solar System Plasma Physics*, eds. L. J. Lanzerotti, C. F. Kennel, E. N. Parker, North Holland Publ. Cy, Amsterdam, III p. 3
Gubchenko, A.M., Zaitsev, V.V.: 1979, *Solar Phys.* **63**, 337
Hjellming, R.M.: 1974, in *Galactic and Extragalactic Radio Astronomy*, ed. G. L. Verschuur and K. I. Kellerman, Springer Verlag, Berlin p. 159
Hjellming, R.M., Gibson, D.M.: 1979, in Radio Physics of the Sun, IAU *Symp.* No. 86, M. R. Kundu and T. E. Gergeley (eds.), p. 209
Hucht, K.A. van der, Bernat, A.P., Kondo, Y.: 1980, *Astron. Astrophys.* **82**, 14
Johnson, H.R.: 1974, Model Atmospheres for Cool Stars, NCAR-TN/STR-95
Kaplan, S.A., Tsytovich, V.N.: 1973, Plasma Astrophysics, Pergamon Press Oxford, p. 22
Kaplan, S.A., Pikel'ner, S.B., Tsytovich, V.N.: 1974, *Phys. Rep.* **15**, 1
Kudritzki, R.P., Reimers, D.: 1978, *Astron. Astrophys.* **70**, 227
Kulygin, V.M., Mikhailovskii, A.B., Tsapelkin, E.S.: 1971, *Plasma Phys.* **13**, 1111
Kuijpers, J.: 1978, *Astron. Astrophys.* **69**, L9
Kuijpers, J.: 1980a, *Astron. Astrophys.* **83**, 201
Kuijpers, J.: 1980b, *Astrophys. J.* **238**, L165
Lamers, H.J.G.L.M.: 1981, *Astrophys. J.* **245**, 593
Lamers, H.J.G.L.M., Rogerson, J.B.: 1978, *Astron. Astrophys.* **66**, 417
Lemons, D.S.: 1977, thesis, College of Williams and Mary, Virginia
Lemons, D.S., Gary, S.P.: 1978, *J. Geophys. Res.* **83**, 1625
Lucy, L.B., Solomon, P.M.: 1970, *Astrophys. J.* **159**, 879
Manheimer, W.M., Boris, J.P.: 1972, *Phys. Rev. Letters* **28**, 659
Manheimer, W.M., Boris, J.P.: 1977, *Comments Plasma Phys. Cont. Fusion* **3**, 15
Morse, D.L., Greenstadt, E.W.: 1976, *J. Geophys. Res.* **81**, 1791
Papadopoulos, K.: 1977, *Rev. Geophys. Space Sci.* **15**, 113
Priest, E.R., Sanderson, J.J.: 1972, *Plasma Phys.* **14**, 951
Rodriguez, P., Gurnett, D.A.: 1975, *J. Geophys. Res.* **80**, 19
Rosenberg, H.: 1976, *Phil. Trans. R. Soc. London A* **281**, 461
Sagdeev, R.Z.: 1966, in *Reviews of Plasma Physics* IV, ed. M. A. Leontovich p. 23
Sagdeev, R.Z.: 1972, Fifth European Conference on Controlled Fusion and Plasma Physics, Grenoble, p. 105
Sanderson, J.J., Uhrig, R.A.: 1978, *J. Geophys. Res.* **83**, 1395
Sherwell, D., Cairns, R.A.: 1977, *J. Plasma Phys.* **17**, 265
Sherwell, D., Cairns, R.A.: 1978, *J. Plasma Phys.* **20**, 265
Snow, T.P., Marlborough, J.M.: 1976, *Astrophys. J.* **203**, L87
Stenzel, R.L.: 1978, *Phys. Fluids* **21**, 99
Swings, J.P., Preston, G.W.: 1978, *Astrophys. J.* **220**, 883
Tend, W. van, Kuperus, M.: 1978, *Solar Phys.* **59**, 115
Tidman, D.A., Krall, N.A.: 1971, Shock Waves in Collisionless Plasmas, Wiley
Tsytovich, V.N., Stenflo, L., Wilhelmsson, H.: 1975, *Physics Scripta* **11**, 251
Vaiana, G.S. et al.: 1980, *Astrophys. J.*(to be published)
Wade, C.M., Hjellming, R.M.: 1971a, *Astrophys. J.* **163**, L 105
Wade, C.M., Hjellming, R.M.: 1971b, *Astrophys. J.* **168**, L 115
Wendker, H.J.: 1978, *Abh. Hamburger Sternwarte* **10**, 3
Wild, J.P., Smerd, S.F.: 1972, *Ann. Rev. Astron. Astrophys.* **10**, 159
Woods, L.C.: 1969, *J. Plasma Phys.* **3**, 435
Woods, L.C.: 1971, *J. Plasma Phys.* **13**, 289